The University of Chicago

A Life-History Approach to the Late Pleistocene Megafaunal Extinction

Wenyun Zuo,* Felisa A. Smith, and Eric L. Charnov

Department of Biology, University of New Mexico, Albuquerque, New Mexico 87131

abstract: A major criticism of the "overkill" theory for the late Pleistocene extinction in the Americas has been the seeming implausibility of a relatively small number of humans selectively killing off millions of large-bodied mammals. Critics argue that early Paleoindian hunters had to be extremely selective to have produced the highly size-biased extinction pattern characteristic of this event. Here, we derive a probabilistic extinction model that predicts the extinction risk of mammals at any body mass without invoking selective human harvest. The new model systematically analyzes the variability in life-history characteristics, such as the instantaneous mortality rate, age of first reproduction, and the maximum net reproductive rate. It captures the body size–biased extinction pattern in the late Pleistocene and precisely predicts the percentage of unexpectedly persisting large mammals and extinct small ones. A test with a global late Quaternary mammal database well supports the model. The model also emphasizes that quantitatively analyzing patterns of variability in ecological factors can shed light on diverse behaviors and patterns in nature. From a macro-scale conservation perspective, our model can be modified to predict the fate of biota under the pressures from both climate change and human impacts.

Keywords: probabilistic extinction model, size-biased late Quaternary extinction, population dynamics, non-size-selective harvest, external mortality rate.

Introduction

The Americas of 13,400 years ago were vastly different from today. Numerous species of large-bodied mammalian herbivores such as mammoths and mastodons, horses and their allies, camelids, oxen and bison, glyptodonts, giant sloths, and other taxa were widespread across both continents (Martin 1967; Alroy 2001; Barnosky et al. 2004; Koch and Barnosky 2006). These megaherbivores were preyed on by large-bodied carnivores such as sabertooth cats, short-faced bears, and the dire wolf. Within a relatively short time, however, some 80% of these large-bodied species were extinct, including all mammals over 600 kg

* Corresponding author; e-mail: wyzuo@unm.edu.

(Lyons et al. 2004). The strikingly size-selective nature of the extinction (Martin 1967; Alroy 1999; Lyons et al. 2004) was completely unprecedented in the evolutionary history of Cenozoic mammals (Alroy 1999, 2001). Determining the cause(s) underlying the abrupt late Pleistocene extinction of megafauna has been difficult and fraught with controversy (Faith and Surovell 2009) largely because it overlaps in timing with both the initial arrival of humans into the Americas and a major climatic transition. The rapidity and the size-biased nature of the extinction lead to the development of the "blitzkrieg" or "overkill" theory (Martin 1967), which attributed the extinction to overharvesting by early Paleoindian hunter-gatherer population. Though this theory has been controversial, it has slowly gained traction as the most parsimonious explanation of the event (e.g., Koch and Barnosky 2006). Even formerly staunch advocates of climate change as the driver have recently concluded that "human impacts probably figured prominently in the extinctions" (Carrasco et al. 2009, p. e8331). However, a continuing criticism of the overkill theory for the late Pleistocene has been the seeming implausibility of a relatively small number of humans killing off millions of animals and the lack of direct archaeological evidence that early Paleoindian hunters preyed on all extinct large-bodied mammal species (e.g., Grayson and Meltzer 2003, 2004; but see Waguespack and Surovell 2003; Surovell and Waguespack 2008). Moreover, opponents have argued that early Paleoindian hunters would have had to be extremely selective to produce such a highly size-biased extinction, and that the economics of foraging theory suggest that such a size-specialized diet would have been energetically unfeasible (Cannon and Meltzer 2004; Byers and Ugan 2005).

While the debate on which process drove the massive late Pleistocene megafaunal extinction is of interest, understanding the underlying mechanism is arguably as important. Currently, a simple general mechanistic model that quantifies the extinction dynamics is lacking; why did some species succumb whereas other species emerged essentially unscathed? Previous models (Alroy 2001; Brook

and Bowman 2005; Charnov and Zuo 2011) suggest that size-biased harvest forces are not necessary to explain the body-mass bias of the extinction. However, Alroy's (2001) complex species-by-species simulation model tested only 41 mammals with body mass larger than 21 kg, and the allometry models (Brook and Bowman 2005; Charnov and Zuo 2011) provided only deterministic extinction thresholds on body size. Here, a probabilistic extinction risk model is derived to explain why there is unexpected persistence of some large taxa and extinction of some small ones despite the size-selective nature of the late Pleistocene extinction. Our model addresses not only the pattern of the size-biased extinction but also underlying mechanism, which previously has been only explained qualitatively (Brook and Bowman 2005; Koch and Barnosky 2006; Charnov and Zuo 2011). Our probabilistic model is built following the deterministic model of Charnov and Zuo (2011) by analyzing variation in life-history characteristics, such as instantaneous mortality rate, age of first reproduction, and the maximum net reproductive rate. Our results account for the gradual rise in extinction risk with body mass (Lyons et al. 2004; Polishchuk 2010) and predict the special life-history characteristics of a species at a given body mass that raise or lower the risk of extinction. Our predictions are consistent with empirical patterns derived from a late Quaternary mammal database (Smith et al. 2003, referred to as "MOM v3.0") that contains a comprehensive set of both extant and extinct species for the Americas.

Model Development

Recently, Charnov and Zuo (2011) derived a simple deterministic threshold model based on the harvest instantaneous mortality rate and the maximum recruitment rate, which points out that the variability around the allometry of background instantaneous mortality rate is one of the most important reasons why some large taxa persist unexpectedly and some small taxa become extinct. A stable animal population necessarily has instantaneous mortality rates that equal recruitment rates. In theoretical macroecological studies, it is a generally accepted assumption that adult instantaneous mortality rates are independent of population size. For large mammals, it is a good approximation; for small mammals, particularly microtines, patterns are more ambiguous. Various studies report density-independent, weakly density-dependent, and delayed density-dependent adult mortality (Krebs 1974; Finerty 1980; Bondrup-Nielsen 1987; Price and Kelly 1994; Ostfeld and Canham 1995). However, for a macro scale, which spans the entire body mass spectrum, such a simplified assumption is justified as it helps us capture the general extinction pattern for all mammals instead of species-specific pattern. Considerable evidence (Fowler 1981, 1987, 1988; Myers et al. 1999; Charnov 1993) supports the density-dependent response for recruitment rates; if a population declines, its recruitment rate increases. A maximum recruitment rate, therefore, will be reached if the population declines dramatically. The population is doomed to extinction if the maximum recruitment rate is less than the adult mortality rate. Charnov and Zuo (2011) derive an extinction threshold, $R_{0\max}e^{-\alpha F}/(1 + F/M) < 1$, where $R_{0\max}$ is the maximum net reproductive rate, $e^{-\alpha F}$ represents the effect of human harvest on juvenile survivorship, α is the age of first reproduction, F is the harvest instantaneous mortality, and M is the background adult instantaneous mortality. This formula captures the effects of hunting on both adult survivorship and on the probability that a newborn will survive to the age of first reproduction. A boundary case can be expressed as $R_{0\max}e^{-C\cdot\alpha M}/(1 + C) = 1$, where C is the threshold of extinction, the value of F/M. The threshold C can be solved numerically via the following equation:

$$\frac{e^{-C\cdot\alpha M}}{1 + C} = \frac{1}{R_{0\max}}. \quad (1)$$

Since $\alpha \propto W^{0.25}$, $M \propto W^{-0.25}$ (where W is body mass), and $R_{0\max}$ is independent of body mass (Charnov 2001; Charnov and Zuo 2011), C is also independent of body mass (eq. [1]).

Therefore, a general life-history rule for harvest mortality caused extinction can be simplified as

$$C < \frac{F}{M}. \quad (2)$$

Figure 1 illustrates Charnov and Zuo's extinction threshold rule (eq. [2]) and also illustrates that the variability in adult instantaneous mortality rates across species at a given body mass determines the extinction probability of species at that mass.

Here a more comprehensive model is derived by integrating the probability distribution of variability in the threshold rule (eq. [2]; Charnov and Zuo 2011), which accounts for the gradual rise in extinction risk with body mass. Assume the harvest mortality rate $F = A_1 \cdot W^\delta$, where δ represents the bias on body mass from harvest and A_1 is harvest mortality strength. When $\delta = 0$, there is no body-size bias of harvesting, whereas when $\delta > 0$, there is increasing harvest mortality for larger-bodied animals. Since $M = A \cdot W^{-0.25}$ (Charnov 2001), where A is background adult mortality strength, the threshold rule ($C < F/M$) can be rewritten as

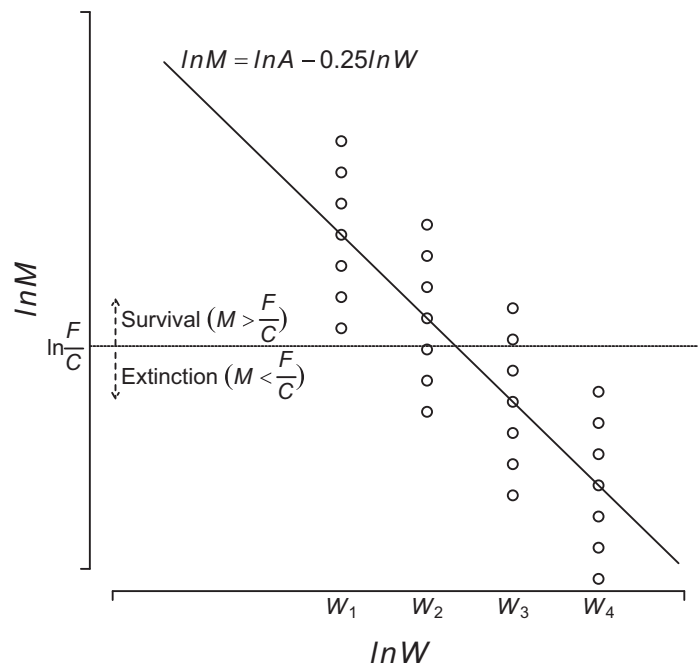$$\ln W > \frac{\ln C + \ln A - \ln A_1}{0.25 + \delta}, \quad (3)$$

Figure 1: The extinction threshold combined with the allometry of adult instantaneous mortality rate (M) generates size-biased extinction. Circles represent species. If the ratio of harvest instantaneous mortality rate (F) and the extinction threshold (C) is larger than M ($F/C > M$), species become extinct. The variability in M among species at a given body mass (W) drives the increase in the extinction probability with $\ln W$. At mass W_1, no species have $\ln M$ that crosses the ratio, (F/C), so none become extinct; at mass W_4, all become extinct. Three of seven become extinct at W_2, five of seven at W_3, and so forth. The M scaling relationship, $\ln M = \ln A - 0.25 \ln W$, derives extinction probability from 0 to 1 with increasing body mass, where A is background adult mortality strength. The variability in M among species at a given body mass turns a deterministic threshold into a probabilistic extinction curve (fig. 3).

which addresses the extinction threshold from the perspective of body mass, where variables A, C, A_1, and δ are all independent of body mass. Equation (3) can be simplified by assigning a variable $x \equiv (\ln C + \ln A - \ln A_1)/(0.25 + \delta)$. If C, A, A_1, and δ are constants across species, the rewritten threshold rule (eq. [3]) is still deterministic. It indicates that any species having a body mass larger than e^x kg will become extinct. However, instead of being constants, C, A, and A_1 are most likely to vary across species. Therefore, equation (3) is no longer deterministic. For a given body mass (W_1), equation (3) ($\ln W_1 > x$) is held with a probability (p), indicating the tendency for a species with body mass W_1 to become extinct. The extinction probability for species with body mass W_1 can be calculated as

$$p(W_1) = \int_{-\infty}^{\ln W_1} g(x)\,dx, \tag{4}$$

where $g(x)$ is a normal distribution of x, combined from lognormal distributions of C and A (fig. 2; see app. A for

further details). For the present, we assume A_1 is a constant.

Results

Our model suggests variation in the background adult instantaneous mortality rate (M), the age of the first reproduction (α), and the maximum net reproductive rate ($R_{0\max}$) at a given body mass are the major reasons why some species succumbed whereas others survived the late Pleistocene extinction event. Equation (4) predicts gradually raised extinction probability with increased body mass as long as $\delta > -0.25$. When we compared model results with the empirically derived extinction probability curves for the late Pleistocene extinction in the Americas we obtained close correspondence, although results differed somewhat for North and South America (fig. 3).

Estimation of the Probability Distribution of x

Based on variation in the background adult instantaneous mortality rate (M), the age of the first reproduction (α), and the maximum net reproductive rate ($R_{0\max}$) at a given
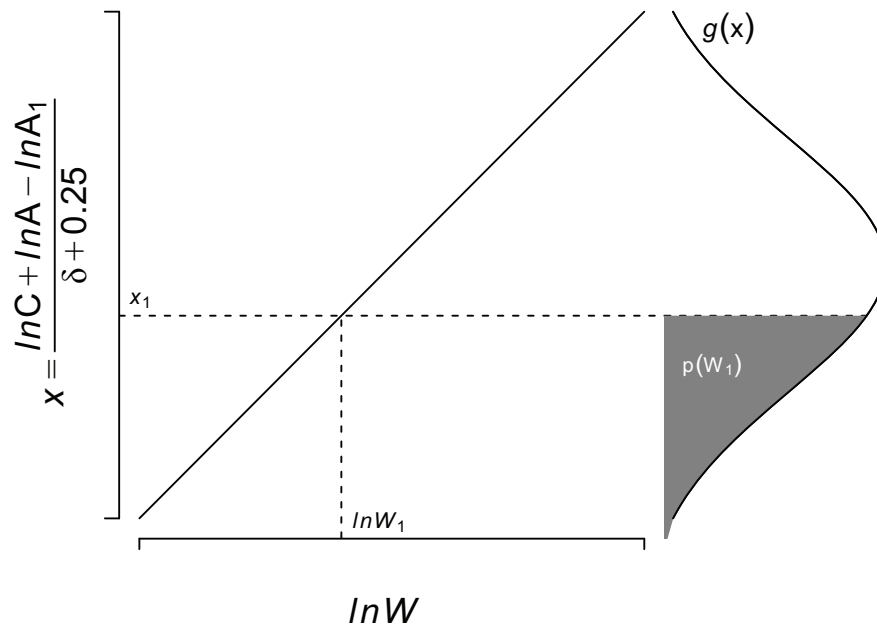
Figure 2: The probability of extinction at a given body mass. The variable, which aggregates background adult mortality strength (A) and extinction threshold (C), has a normal distribution, $g(x)$. The area under $g(x)$ up to x_1 ($x_1 = \ln W_1$) gives the proportion of species with body mass W_1 that become extinct; $p(W_1)$ is the extinction probability for species with body mass W_1.

body mass, the estimated probability distribution of x, $g(x)$, is normal, with a mean of $-(1.08 + \ln A_1)/(0.25 + \delta)$ and a standard deviation of $0.60/(0.25 + \delta)$ (app. A).

Estimation of Harvest Mortality Rate in Late Pleistocene

Figure 2 illustrates that species will have a 50% probability of becoming extinct ($p = .5$), if their logarithmic adult body size equals the mean of $g(x)$, which gives $\ln W_{p=.5} = -(1.08 + \ln A_1)/(0.25 + \delta)$. Since $F = A_1 \cdot W^\delta$, the harvest mortality rate for species at the body mass associated with $p = .5$ can be computed as $F_{W_{p=.5}} = e^{-1.08} \cdot W_{p=.5}^{-0.25}$. The empirical extinction risk for species at any body mass was calculated from an updated version of the MOM data set (Smith et al. 2003) using logistic regression following the lead of Polishchuk (2010). We include only terrestrial, nonvolant mammals in our analysis (e.g., bats [Chiroptera] and pinnipeds [Odobenidae, Otariidae, and Phocidae] are excluded). Data suggest that mammals with a body mass of ~60 kg (95% confidence interval [CI]: 23–219 kg, χ^2 $p < .0001$) had a 50% chance of extinction during the terminal Pleistocene (fig. 3). Therefore, our model estimates the harvest mortality rate body mass associated with 50% extinction probability, $F_{W_{p=.5}} = 0.122$, at late Pleistocene.

Empirical Test of the Model

Our model (eq. [4]) quantitatively demonstrates that an additional, but not size-selective ($\delta = 0$), harvest mortality is sufficient to have resulted in the strongly size-biased extinction for the Americas overall. For North America, there is excellent quantitative agreement between the empirical data and our model predictions (fig. 3). While results for North America are statistically indistinguishable from the results as a whole, South America is somewhat different (fig. 3C). Not only is the fitted slope of logistic regression nearly twice as steep as that for North America (1.23 vs. 0.66; fig. 3B, 3C) but applying our model without invoking any size bias ($\delta = 0$) results in a slope that lies outside the 95% confidence interval of the empirical extinction risk curve. To generate a theoretical curve consistent with the empirical curve in South America, a slight size bias ($\delta = 0.15$) must be incorporated for harvest mortality.

Discussion

Our theory quantitatively illustrates that it is not necessary to invoke size-biased harvest from early Paleoindian hunters to produce a highly size-biased pattern of extinction. Rather, it simply requires that the added harvest mortality overpowers the increased recruitment that is normally pre-
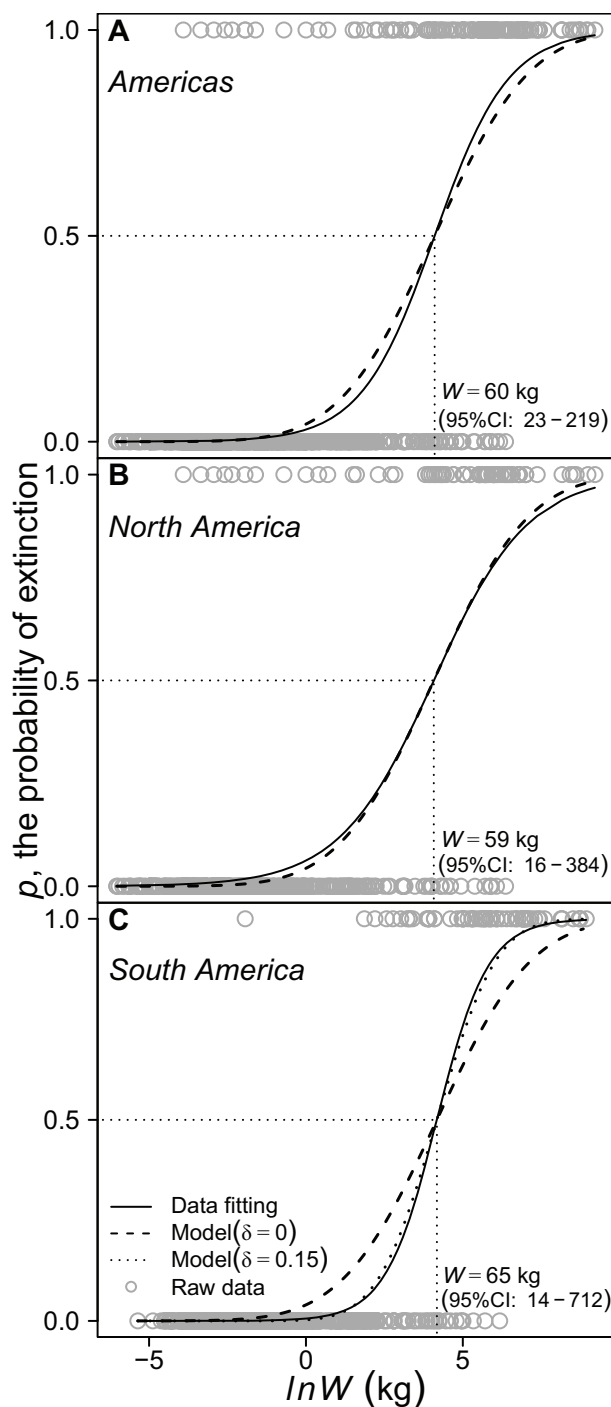
Figure 3: Empirical and model predicted extinction probability (*p*) curves versus ln *W* for late Pleistocene mammals. Empirical data from Smith et al. (2003); extinct species have *p* = 1 and extant species *p* = 0. Data are fitted by logistic regression using the statistical program R (R Development Core Team 2009) to get an empirical extinction probability curve. *A*, For both North and South America, the empirical extinction probability curve has a fitted slope of 0.85 (95% confidence interval [CI]: 0.73–0.97, χ^2 *p* < .0001) based on all 1,323 species. Our theory matches this distribution without invoking size-biased harvest mortality ($\delta = 0$). *B*, In North America, the empirical slope = 0.66 (95% CI: 0.54–0.79, χ^2 *p* < .0001) based on 572 species. Again, the theory matches this distribution without invoking size bias ($\delta = 0$). *C*, In South America, the empirical slope = 1.23 (95% CI: 0.95–1.51, χ^2 *p* < .0001) based on 775 species. Here, a slight size bias ($\delta = 0.15$) is required for the theory to match data. Our model predicted slopes are 0.76 without size bias and 1.22 with size bias ($\delta = 0.15$). There are 24 species shared by both North and South America. See appendix B for further details on calibrating the theoretical extinction probability curve.

sent as population size approaches zero. Our model almost perfectly recapitulates the empirical data for Americas (fig. 3).

Because most scientists view the late Quaternary extinction in the New World as part of a single event (Martin 1967; Martin and Klein 1989; Alroy 1999, 2001), we combined data for both continents in our analysis (fig. 3). When we examined the continents independently, however, we found some intriguing differences between North and South America (fig. 3*B*, 3*C*). Only in South America was a size-biased ($\delta = 0.15$) harvest mortality necessary for the model to capture the empirical extinction curve. Whether this was a signal of a change in hunting patterns or the result of poorer-quality data is unclear. Fossil information for the late Quaternary of South America is potentially less robust because of reduced sampling and other taphonomic issues. For example, smaller mammals tend to be underrepresented because of a historical lack of screening for small bones, and they may even be underrepresented in the characterization of the modern fauna (Smith et al. 2003). If, however, the predicted size-biased harvest mortality of South America was not the result of noisy data, it raises some interesting questions. What sort of harvest forces would invoke a size bias in South America but not North America? Did early Paleoindian hunters become more efficient in their hunting strategies? Did they "learn" to prefer large-bodied prey by the time they reached South America? While early hunters may have harvested prey indiscriminately on first reaching the New World, perhaps the naive nature of the animals they encountered allowed them to begin concentrating on large-bodied and more cost-effective animals as they migrated southward. Alternatively, perhaps the difference in openness of habitats altered the susceptibility of prey in South America, making larger animals more visible on the landscape.

The data displayed in figure 3 clearly show that there is no deterministic threshold for extinction with respect to body mass. The variance in *g*(*x*), representing the probability distribution of *x*, determines the steepness of the gradually raising extinction probability with body mass. Reduced variance of *g*(*x*) leads to extinction probability

rising sharply with body mass; greater variance to a slower rise. The variability in the adult mortality strength (A) is the most important component influencing the variance of $g(x)$. Thus, rather than invoking size-biased harvest in South America, the steeper extinction curve might be caused by reduced variability in the adult mortality strength (A) for South American mammals in the late Pleistocene. We have not implicitly included the variability in harvest mortality strength (A_1) because there has been no a priori basis for characterizing it. However, according to the model, any variability in the harvest mortality rate increases the overall variance of $g(x)$, thus reducing the steepness in the predicted extinction probability curve.

Scaling relationships of background adult instantaneous mortality ($M = A \cdot W^{-0.25}$) and harvest instantaneous mortality rate ($F = A_1 \cdot W^{\delta}$) determine the size-biased extinction pattern. If the sum of the two exponents is larger than zero, $0.25 + \delta > 0$, extinction acts heavily on large-sized mammals. Conversely, if $0.25 + \delta < 0$, extinction risk is higher for small-sized mammals. If $0.25 + \delta = 0$, it is simply indicates that all mammals have the same extinction probability regardless of body mass.

Our model predicts how large harvest mortality has to be to result in extinction of 50% of species for a given body mass ($F_{W_{p=.5}} = e^{-1.08} \cdot W_{p=.5}^{-0.25}$). If harvesting was not size biased ($\delta = 0$), the harvest mortality for species at $W_{p=.5}$ is also the harvest mortality for all species regardless of body mass. If $\delta \neq 0$, the harvest mortality for a given species can be estimated by $F = F_{W_{p=.5}} W^{\delta} / W_{p=.5}^{\delta}$. However, the absolute value of the estimated harvest mortality here is less important, because it is unclear how much difference remains in life-history data between modern mammals and mammals at later Pleistocene.

It is straightforward to examine targeted harvest pressure of particular ages. Currently, our theory assumes harvest mortality acts on all age groups from juveniles to adults, but it can be modified to target only adults, as is commonly done in the fishery literature. Such a modification of equation (1) gives an analytic solution of $C = R_{0\max} - 1$ for the extinction threshold. Substituting $C = R_{0\max} - 1$ into equation (3) gives an extinction threshold from the perspective of body mass as $\ln W > [\ln (R_{0\max} - 1) + \ln A - A_1]/(0.25 + \delta)$. Therefore, the estimated probability distribution, $g(x)$, is no longer dependent on the age of first reproduction (α). It only depends on the background adult instantaneous mortality rate (M) and the maximum net reproductive rate ($R_{0\max}$). It has a mean of $-(0.38 + \ln A_1)/(0.25 + \delta)$ and a standard deviation of $0.61/(0.25 + \delta)$. Equation (4) still gives the extinction probability for any body mass. The changed mean of $g(x)$ implies that about twofold of estimated harvest mortality ($F_{W_{p=.5}} = e^{-0.38} \cdot W_{p=.5}^{-0.25}$) is required to cause the similar pattern of later Pleistocene extinction in Americas.

Pleistocene extinctions in Australia are also biased toward large-sized animals but with a much steeper slope than for other continents (Polishchuk 2010). We cannot explore the event in Australia precisely because of the lack of demographic data for marsupials, which vary in important ways from Eutherian mammals (Hamilton et al. 2011). However, the steeper slope characteristic for Australia may suggest a smaller variance of $g(x)$, which might suggest lower variation in adult mortality strength (A), age of first reproduction (α), or the maximum net reproductive rate ($R_{0\max}$). Alternatively, δ may be every large, which implies a strong size bias from the harvest mortality.

The theory reemphasizes that species at a given body mass with relatively low mortality rates (M) and/or low maximum net reproductive rates ($R_{0\max}$) are more likely to suffer extinction. These are species lying below the solid line in figure 1 or which have small x in figure 2. It is difficult to test this directly because adult mortality rate, age of first reproduction and the maximum net reproductive rate are unknown for extinct species. Our theory also raises an important perspective that systematically analyzing variations around canonical curves or values can provide an insight to diverse behaviors or responses in nature. From a conservation perspective, our model may help predict the future of biota under pressure from both climate change and habitat alteration.

Acknowledgments

APPENDIX A

Estimating $g(x)$

The term $g(x)$ presents the probability distribution of x, where $x \equiv (\ln C + \ln A - \ln A_1)/(0.25 + \delta)$. If C, A, A_1,

and δ are constants across species, x is consequently a constant. However, instead of being constants, C, A, and A_1 more likely vary across species. Therefore, x is also a variable with a probability distribution. We assume that harvest mortality strength (A_1) and the size-bias parameter (δ) are constants, because we have no a priori basis for characterizing them. Therefore, the probability distribution of $x \equiv (\ln C + \ln A - \ln A_1)/(0.25 + \delta)$ can be characterized by the distribution of $\ln C$ and $\ln A$.

The distribution of logarithmic background adult instantaneous mortality strength ($\ln A$) derives from variation of the residuals around the allometry of the adult instantaneous mortality rate (M), obtained from Purvis and Harvey's data set (Purvis and Harvey 1995; Charnov and Zuo 2011). The obtained distribution of residuals is not significantly different from a normal distribution (D'Agostino-Pearson test: df = 56, $p = .332$). The standard deviation for the distribution of $\ln A$ is 0.59 and its mean is −0.38.

The distribution of the logarithmic threshold of extinction ($\ln C$) is slightly complicated. Since, there is only a numerical solution for equation (1), $e^{-C \cdot \alpha M}/(1 + C) = 1/R_{0\max}$, the variation in $\ln C$ across species can be calculated numerically as a function of the background adult instantaneous mortality rate (M), age of first reproduction (α), and the maximum net reproductive rate ($R_{0\max}$). The value of $\alpha \cdot M$ is obtained from Purvis and Harvey's data set (Purvis and Harvey 1995; Charnov and Zuo 2011) and is significantly different from a normal distribution (D'Agostino-Pearson test: df = 53, $p < .001$), but $\ln(\alpha \cdot M)$ is not (D'Agostino-Pearson test: df = 53, $p = .370$). The value of $\ln(\alpha \cdot M)$ has a mean of −0.62 with an SD of 0.41. The maximum net reproductive rate $R_{0\max}$ is around 2~3 and is independent of body size (Fowler 1981, 1987, 1988; Charnov 1993). The values of $R_{0\max}$ are small because juvenile survivorship, S_α, cannot increase much in mammals and the number of daughters produced per mother per unit time, b, is more or less invariant. Term S_α is already quite high (estimated to be 0.3~0.4; Charnov 1993), and b is expected to be highly dependent on adult body size, which is not expected to change much as population size N changes. If b is fixed, $R_{0\max}$ can only reflect the increase in S_α at low N. The maximum S_α could be 1. In reality, the value of the maximum S_α is likely to be far below 1 (e.g., 0.6~0.8), so $R_{0\max}$ may be less than 2~3. To explore more of the uncertainty of $R_{0\max}$, we assume two cases. Case I: we consider $R_{0\max}$ is centered at 2 with a distribution such that the lower bound of the 99% confidence interval does not reach too close to 1. We assume that $\ln R_{0\max}$ is normal with mean of 0.69 ($R_{0\max} = 2$) and standard deviation of 0.15, which places the 99% confidence interval between 0.30 and 1.09, so that $R_{0\max}$ ranges from 1.35 to 2.97. Case

II: we assume $R_{0\max} = 2$ is a constant and the same for all species. To calculate C, a random value of $\ln(\alpha \cdot M)$ is picked from its normal distribution, and so is a random value of $\ln R_{0\max}$ (picked from its normal distribution if case I; equals 0.69 in case II). A total of 10,000 values of $\ln C$ are calculated according to equation (1), which are used to estimate the distribution of $\ln C$. Out of 10,000 values of $\ln C$, 1,000 of them are picked randomly for testing if $\ln C$ follows normal distribution. The D'Agostino-Pearson test shows that $\ln C$ is significantly different from a normal distribution (df = 999, $p < .001$).

The distribution of $\ln C + \ln A$ is generated numerically by randomly picking 10,000 such sums by combining the distributions of appropriate components, $\ln C$ and $\ln A$, to produce a continuous distribution for the sum. However, $\ln A$ and $\alpha \cdot M$, a component in equation (1) for calculating $\ln C$, slightly covary (Cov = 0.078; data set from Purvis and Harvey 1995). Therefore, we cannot calculate $\ln C$ and $\ln A$ independently; rather, $\ln C$ and $\ln A$ have to be computed simultaneously. The distribution of $\ln C + \ln A$ is computed from a normal distribution of $\ln R_{0\max}$ (if case I; fixed values, as 0.69 if case II) and a multivariable normal distribution of $\ln A$ and $\alpha \cdot M$. Total 10,000 of $\ln C + \ln A$ are calculated to estimate the distribution of $\ln C + \ln A$ for each case, respectively (case I with varied $R_{0\max}$ and case II with fixed $R_{0\max}$). A D'Agostino-Pearson test demonstrates that $\ln C + \ln A$ is not significantly different from a normal distribution for both cases (case I: df = 999, $p = .338$ with mean of −1.08 and SD of 0.60; case II: df = 999, $p = .349$ with mean of −1.08 and SD of 0.54). Substituting the distribution of $\ln C + \ln A$ into $x \equiv (\ln C + \ln A - \ln A_1)/(0.25 + \delta)$ reveals that $g(x)$ is normal with a mean as $-(1.08 + \ln A_1)/(0.25 + \delta)$, SD as $0.60/(0.25 + \delta)$ (case I: varied $R_{0\max}$) and $0.54/(0.25 + \delta)$ (case II: fixed $R_{0\max}$). All the computations were performed in R (R Development Core Team 2009).

APPENDIX B

Calibrating the Extinction Probability Curve

We define that harvest mortality $F = A_1 \cdot W^\delta$, where δ is the body mass bias of the harvest mortality and A_1 is harvest mortality strength. Therefore, $\ln A_1$ is available if we can estimate the harvest mortality. Our model estimates the harvest mortality rate body mass associated with 50% extinction probability, $F_{W_{p=.5}} = e^{-1.08} \cdot W_{p=.5}^{-0.25}$. Therefore, $\ln A_1 = \ln F_{W_{p=.5}} - \delta \cdot \ln W_{p=.5}$. The empirical extinction risk derived from logistic regression of the MOM data set (Smith et al. 2003) shows that mammals of about 60 kg (95% CI: 23–219 kg, χ^2 $p < .0001$) had a 50% chance of extinction during the terminal Pleistocene, $W_{p=.5} = 60$ kg

(fig. 3). From $F_{W_{p=.5}} = e^{-1.08} \cdot W_{p=.5}^{-0.25}$, we get $F_{W_{p=.5}=60\,\text{kg}} \approx 0.122$. For non-size-selective harvest ($\delta = 0$), $\ln A_1 = -2.10$, which gives the mean of $g(x)$, $-(1.08 + \ln A_1)/(0.25 + \delta) = 4.06$.

Literature Cited

Alroy, J. 1999. The fossil record of North American mammals: evidence for a Paleocene evolutionary radiation. Systematic Biology 48:107–118.

———. 2001. A multispecies overkill simulation of the end-Pleistocene megafauna mass extinction. Science 292:1893–1896.

Barnosky, A. D., P. L. Koch, R. S. Feranec, S. L. Wing, and A. B. Shabel. 2004. Assessing the causes of late Pleistocene extinctions on the continents. Science 306:70–75.

Bondrup-Nielsen, S. 1987. Demography of *Clethrionomys gapperi* in different habitats. Canadian Journal of Zoology 65:277–283.

Brook, B. W., and D. M. J. S. Bowman. 2005. One equation fits overkill: why allometry underpins both prehistoric and modern body size-biased extinctions. Population Ecology 47:137–141.

Byers, D. A., and A. Ugan. 2005. Should we expect large game specialization in the late Pleistocene? an optimal foraging perspective on early Paleoindian prey choice. Journal of Archaeological Science 32:1624–1640.

Cannon, M. D., and D. J. Meltzer. 2004. Early Paleoindian foraging: examining the faunal evidence for large mammal specialization and regional variability in prey choice. Quaternary Science Reviews 23:1955–1987.

Carrasco, M. A., A. D. Barnosky, and R. W. Graham. 2009. Quantifying the extent of North American mammal extinction relative to the pre-anthropogenic baseline. PLoS ONE 4:e8331.

Charnov, E. L. 1993. Life history invariants. Oxford University Press, New York.

———. 2001. Evolution of mammal life histories. Evolutionary Ecology Research 3:521–535.

Charnov, E. L., and W. Zuo. 2011. Human hunting mortality threshold rules for extinction in mammals (and fish). Evolutionary Ecology Research 13:431–437.

Faith, J. T., and T. A. Surovell. 2009. Synchronous extinction of North America's Pleistocene mammals. Proceedings of the National Academy of Sciences of the USA 106:20641–20645.

Finerty, J. P. 1980. The population ecology of cycles in small mammals. Yale University Press, New Haven.

Fowler, C. W. 1981. Density dependence as related to life history strategy. Ecology 62:602–610.

———. 1987. A review of density dependence in populations of large mammals. Pages 401–441 *in* H. Genoways, ed. Current mammalogy. Plenum, New York.

———. 1988. Population dynamics as related to rate of increase per generation. Evolutionary Ecology 2:197–204.

Grayson, D. K., and D. J. Meltzer. 2003. A requiem for North American overkill. Journal of Archaeological Science 30:585–593.

———. 2004. North American overkill continued? Journal of Archaeological Science 31:133–136.

Hamilton, M. J., A. D. Davidson, R. M. Sibly, and J. H. Brown. 2011. Universal scaling of production rates across mammalian lineages. Proceedings of the Royal Society B: Biological Sciences 278:560–566.

Koch, P. L., and A. D. Barnosky. 2006. Late Quaternary extinctions: state of the debate. Annual Review of Ecology, Evolution, and Systematics 37:215–250.

Krebs, C. J. and J. H. Myers. 1974. Population cycles in small mammals. Advances in Ecological Research 8:267–399.

Lyons, S. K., F. A. Smith, and J. H. Brown. 2004. Of mice, mastodons and men: human-mediated extinctions on four continents. Evolutionary Ecology Research 6:339–358.

Martin, P. S. 1967. Pleistocene extinctions: the search for a cause. Pages 75–120 *in* P. S. Martin and H. E. Wright Jr., eds. Yale University Press, New Haven, CT.

Martin, P. S., and R. G. Klein. 1989. Quaternary extinctions: a prehistoric revolution. University of Arizona Press, Tucson.

Myers, R. A., K. G. Bowen, and N. J. Barrowman. 1999. Maximum reproductive rate of fish at low population sizes. Canadian Journal of Fisheries and Aquatic Sciences 56:2404–2419.

Ostfeld, R. S., and C. D. Canham. 1995. Density-dependent processes in meadow voles: an experimental approach. Ecology 76:521–532.

Polishchuk, L. V. 2010. The three-quarter-power scaling of extinction risk in Late Pleistocene mammals, and a new theory of the size selectivity of extinction. Evolutionary Ecology Research 12:1–22.

Price, M. V, and P. A. Kelly. 1994. An age-structured demographic model for the endangered Stephens' kangaroo rat. Conservation Biology 8:810–821.

Purvis, A., and P. H. Harvey. 1995. Mammal life-history evolution: a comparative test of Charnov's model. Journal of Zoology (London) 237:259–283.

R Development Core Team. 2009. R: a language and environment for statistical computing. R Foundation for Statistical Computing, Vienna. http://www.r-project.org.

Smith, F. A., S. K. Lyons, S. K. M. Ernest, K. E. Jones, D. M. Kaufman, T. Dayan, P. A. Marquet, J. H. Brown, and J. P. Haskell. 2003. Body mass of late Quaternary mammals. Ecology 84:3403, http://dx.doi.org/10.1890/02-9003

Surovell, T. A., and N. M. Waguespack. 2008. How many elephant kills are 14? Clovis mammoth and mastodon kills in context. Quaternary International 191:82–97.

Waguespack, N. M., and T. A. Surovell. 2003. Clovis hunting strategies, or how to make out on plentiful resources. American Antiquity 68:333–352.